Λ-Hyperon Production via the $pp \longrightarrow pK^+\Lambda$ Reaction 2 MeV above Threshold.

J.T. Balewski[1], A. Budzanowski[1], H. Dombrowski[2], C. Goodman[3], D. Grzonka[4], J. Haidenbauer[4], C. Hanhart[4], L. Jarczyk[5], M. Jochmann[6], A. Khoukaz[2], K. Kilian[4], M. Köhler[6], A. Kozela[1], T. Lister[2], R. Maier[4], P. Moskal[5], W. Oelert[4], D. Prasuhn[4], C. Quentmeier[2], R. Santo[2], G. Schepers[2], U. Seddik[7], T. Sefzick[4], J. Smyrski[5], M. Sokołowski[5], A. Strzałkowski[5], M. Wolke[4], P. Wüstner[6]

[1] Institute of Nuclear Physics, Cracow, Poland

[2] IKP, Westfälische Wilhelms–Universität, Münster, Germany

[3] IUCF, Bloomington, Indiana, USA

[4] IKP, KFA Jülich, Germany

[5] Institute of Physics, Jagellonian University, Cracow, Poland

[6] ZEL, KFA Jülich, Germany

[7] NRC, Atomic Energy Authority, Cairo, Egypt

Abstract: The $pp \longrightarrow pK^+\Lambda$ reaction was measured at COSY with a proton beam momentum of 2.345 GeV/c, i.e. with an excess energy of 2 MeV above threshold. The total cross section was determined to be 8.2 $\pm$ 1.8 nb. The present data point close to the production threshold indicates, that existing phenomenological parametrizations of the total kaon production cross section are insufficient.

PACS: 14.20.Jn, 14.40.Aq
Keywords: threshold measurement, strangeness production,
final state interaction, baryon-hyperon scattering length

1 Introduction

The associated strangeness production is an excellent tool to study reaction mechanisms and hadron dynamics in the nonperturbative region of strong interaction physics. Such investigations might relate quark model concepts to descriptions in terms of mesonic and nucleonic degrees of freedom. The (s-$\overline{s}$) quark pair creation provides a clean signal of the reaction dynamics since there are no strange valence quarks in the proton-proton entrance channel. Variation of the experimental input parameters such as projectile-target combinations, beam momenta, and incident spin states provides complementary information needed for a complete analysis.

Inclusive Λ-hyperon production experiments [1] using the high energy (200 GeV/c) proton beam have shown that spin effects are more important than predicted by perturbative QCD calculations. Spin effects are also being investigated at much lower beam momenta (in the range of 3.5 GeV/c) in the DISTO collaboration at Saturne [2] studying $\vec{p}p \longrightarrow pK^+(\Lambda/\Sigma^\circ)$ production including the decay properties of the hyperon. In addition, complementary information will come from two other experiments investigating associated strangeness production. These are the PS185 collaboration at LEAR [3], using the proton-antiproton interaction to study the associated strangeness production in the final hyperon-antihyperon channel, and the non-hadronic photon induced associated strangeness production ($\gamma p \rightarrow K\Lambda$) [4], which eliminates the final state interaction between baryons. A comprehensive analysis of the different experimental measurements should provide a coherent picture.

In all hadronic processes the basic quark or boson exchange dynamics are distorted and partly hidden by strong initial and final state distortions. A chance to disentangle ISI and FSI effects from the elementary dynamics might be to study the same (s-$\bar{s}$) dissociation in experiments with different hadronic surroundings. The dominant N-Λ coupling strength has to be understood before questions of the reaction mechanism can be addressed. Additionally, the K-meson rescattering on a nucleon should be considered.

Studying the reaction $pp \longrightarrow pK^+\Lambda$ near threshold simplifies the theoretical analysis because only one or very few partial waves are present. Also, since all the reaction products go forward in a narrow cone, the acceptance of the detectors can be near 100%. Existing data are meager and not close to threshold. The total cross section at p_b=2.81 GeV/c, corresponding to excess energy Q_{CM}=158 MeV, is given by Flickinger [5] and is based on 11 events observed in a bubble chamber at the BNL in 1962. The latest data from Saturne [6] at p_b=3.1 GeV/c (Q_{CM}=252 MeV) include various reaction channels, since only the differential cross section for K^+ was measured inclusively.

A first step towards a systematic investigation of the associated strangeness production, studied at the proton synchrotron COSY at the KFA Jülich, has been done at COSY-TOF [7] using 2.5 and 2.75 GeV/c proton beam momentum. Data analysis of that experiment is in progress. Here we report the first exclusive measurement close to threshold at p_b=2.345 GeV/c (Q_{CM}=2 MeV) performed at the COSY-11 [8] facility.

2 Experimental method

At a beam momentum (p_b) of 2.339 GeV/c, the $pp \longrightarrow pK^+\Lambda$ channel opens and at 2.57 GeV/c there is the next threshold for the $pp \longrightarrow pK^+\Sigma^\circ$ reaction. A beam momentum of 2.345 MeV/c was chosen for the present experiment, only Q_{CM}=2 MeV above the Λ production threshold. There the acceptance for prompt K^+ and p is very high and the Σ° production channel is not yet open.

A cluster target was installed in front of a normal C-type COSY bending magnet. The diameter of the hydrogen cluster beam is about 9 mm with a density of $5 \cdot 10^{13}$ atoms/cm^3. An overall average luminosity of $7 \cdot 10^{29}$ cm^{-2} s^{-1} was determined from elastically scattered protons. The internal proton beam from the synchrotron COSY Jülich [9] had an emittance of ε = 2.3 mm mrad, a momentum resolution of

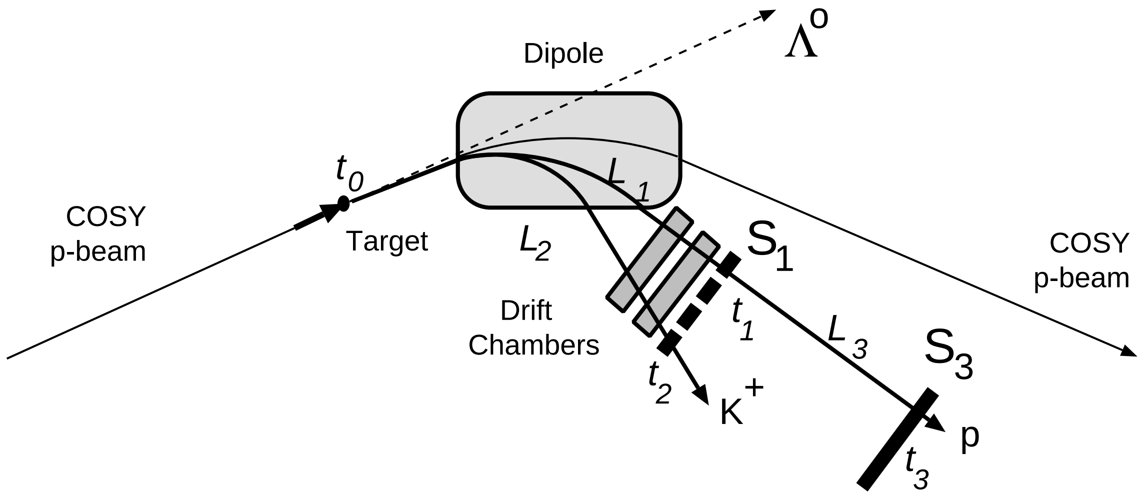

Figure 1: Experimental layout for the $pp \longrightarrow pK^+\Lambda$ measurement.

$\Delta p/p < 10^{-3}$ and an intensity of about $3 \cdot 10^{16}$ particles/sec.

The complete kinematical reconstruction of the $pK^+\Lambda$ events is obtained employing a system of a magnetic field, drift chambers and scintillators described in detail in [8]. As shown schematically in fig. 1, charged ejectiles are deflected in the dipole magnet and detected in the drift chambers. The momentum vector of the proton $\mathbf{p}$ is reconstructed from backtracking through the magnetic field to the nominal target position. Two fast scintillators S1 and S3 measure the time of flight (TOF) over the distance of $L_3 = 9\ m$ and enable the mass identification for charged ejectiles. Using the relation

$$m = \mid \mathbf{p} \mid / (\beta \cdot \gamma), \tag{1}$$

a very good separation between protons and pions is obtained as shown in fig. 2. Charged particles (A) are accepted as protons, if the measured TOF differs from the calculated $TOF(\beta(\mathbf{p}_p, m_p), L_3)$ by less than 4 ns, resulting in the grey area, displayed in the fig. 2.

For the kaon identification a similar technique was used with the S1 scintillator as the stop detector for the TOF measurement. The start was estimated from proton data by calculating the time at which the reaction took place: $t_0 = t_1 - L_1/\beta(proton)$. Figure 3 shows a distribution of squared invariant mass of a particle (B) detected in coincidence with the proton. In addition to the large signals from protons and pions, clear signals produced by K^+ particles with a peak to background ratio of about 2:1 can be seen.

Energy and momentum conservation fixes the four-momentum of the unmeasured particle, i.e. the expected Λ-hyperon .

The final identification of the $pp \longrightarrow pK^+\Lambda$ events is shown in fig 4. Only events of the type $pp \longrightarrow pBC$ were considered. The squared invariant mass of the particle B (expected K^+) and missing mass of the particle C (expected Λ-hyperon) are plotted with respect to each other. A clear enhancement at the mass region (m_B, m_C)=(m_{K^+}, m_Λ) can be seen in part a) of the figure. The m_C^2 of the $pp \longrightarrow pK^+C$ events, selected as indicated by the dashed lines in fig. 4a, is plotted in fig. 4b. Assuming

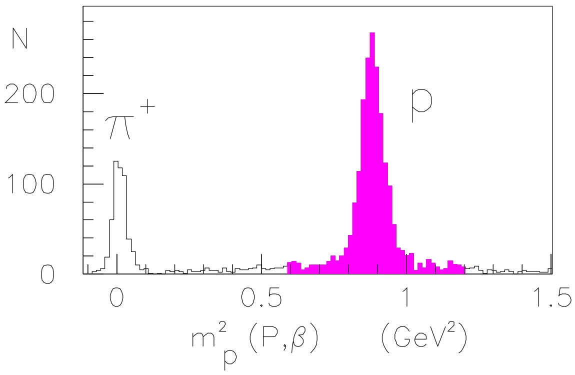

Figure 2: Squared invariant mass (m_p^2) for particles passing through the scintillators S_1 and S_3.

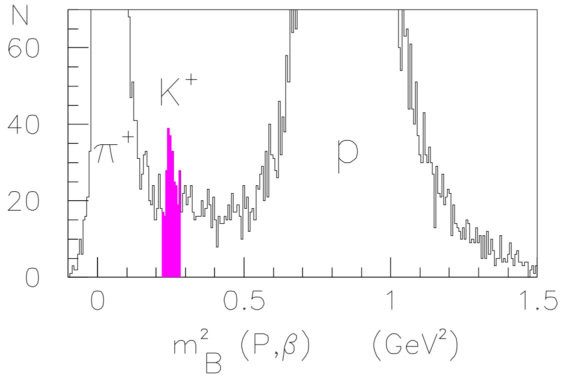

Figure 3: Squared invariant mass of the particle B detected in coincidence with a proton.

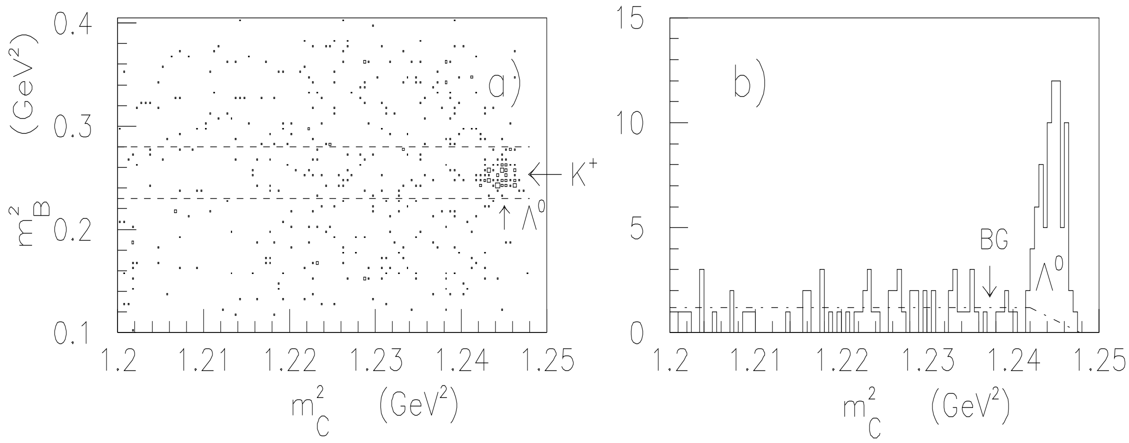

Figure 4: a) Squared invariant mass of the particle B versus the squared missing mass of the (pK^+) system. b) Events from the area between the dashed lines in fig. a) were projected onto the x-axis.

a background distribution as indicated by the dashed line, 69 $pp \longrightarrow pK^+\Lambda$ events were identified, with an uncertainty of 7 events due to the background subtraction. The peak centered at 1.116±0.002 GeV in fig. 4b is in very good agreement with the known mass of the Λ-hyperon . Its full width at half maximum is $\sim$ 1 MeV.

Acceptance studies have been done with the Monte-Carlo method, using a generator of the $pp \longrightarrow pK^+\Lambda$ events with a phase space distribution in the center-of-mass system (CMS). Ejectiles were transported through the magnetic field, drift chambers and scintillators. The response of the detectors was simulated and events were reconstructed with the same algorithm as used for the real data.

The geometrical acceptance for prompt p and K^+ was determined to be 23%. In addition, the decay of about 67% of the K^+ particles before reaching the scintillator S1 decreases the overall detection efficiency to $\eta = 0.075 \pm 0.004$.

The grey area in fig. 5 shows the acceptance of the COSY-11 facility for horizontal momentum vectors of positively charged reaction products. The momentum range of p and K^+ particles, as given by the reaction kinematics, are indicated. All these momenta are accepted in the horizontal plane. The vertical

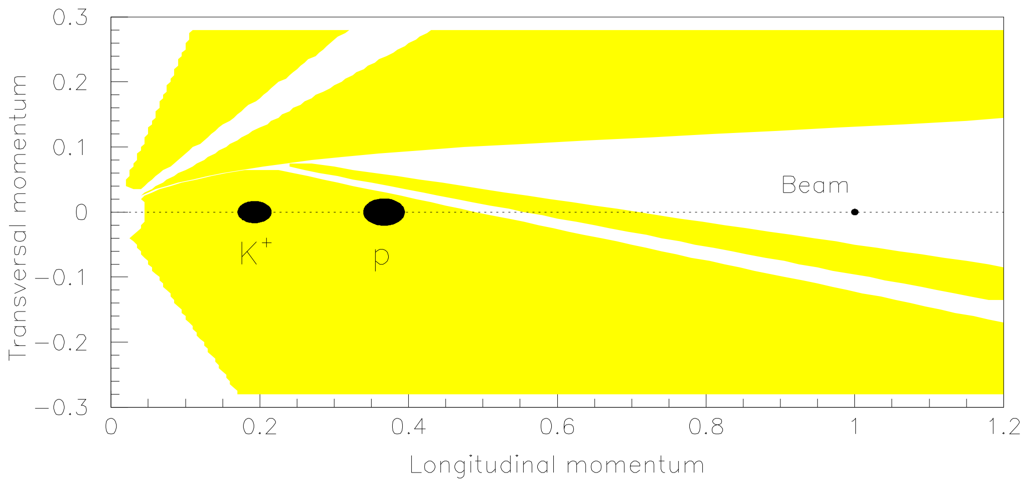

Figure 5: Geometrical acceptance of the COSY-11 facility for positively charged particles, as function of the longitudinal and transversal ejectile momenta, in units relative to the beam momentum. The kinematical position of the beam momentum and ranges of the momenta for K^+ and p from $pp \longrightarrow pK^+\Lambda$ reaction at p_b=2.345 GeV/c are shown.

acceptance limitation is caused by the narrow dipole gap and decreases as the threshold is approached. Thus, very close to threshold this magnetic facility enables the detection of coincident reaction products with 100% geometrical acceptance, which helps in case of small cross sections.

3 Results and discussion

The time integrated luminosity was obtained by measuring simultaneously pairs of elastically scattered protons. The normalization is based on values of the elastic differential cross section given in ref. [10] and [11] for the nearby momenta p_b=2.32, 2.36 and 2.40 GeV/c. The SAID [12] predictions were not used, since solution FA95 overestimates the existing experimental data by 50%. The integrated luminosity was L·T=$(113 \pm 17) \cdot 10^{33} cm^{-2}$.

The final total cross section for the $pp \longrightarrow pK^+\Lambda$ reaction at a beam momentum of $p_b = 2.345 \pm 0.002$ GeV/c is

$$\sigma = N_{pK^+\Lambda}/(\eta \cdot L \cdot T) = 8.2 \pm 1.8 \; nb, \tag{2}$$

The error includes the following uncertainties: statistical 12%, background subtraction 10%, detection efficiency 5% and luminosity 15%.

In order to discuss the energy dependence of the K^+ production cross section close to threshold a model similar to that used for the $pp \rightarrow pp\pi^\circ$ production [13] is tested at first.

The Lorentz invariant form of the total cross section for the 3-body reaction can be found, e.g. in Ref [14]. Assuming that both the $N\Lambda$ system and the kaon (relative to $N\Lambda$) are in S-wave states, the cross section formula simplifies to

$$\sigma = \frac{const}{p_b} \int_0^{q_{max}} |M|^2 \cdot p \cdot q^2 dq. \tag{3}$$

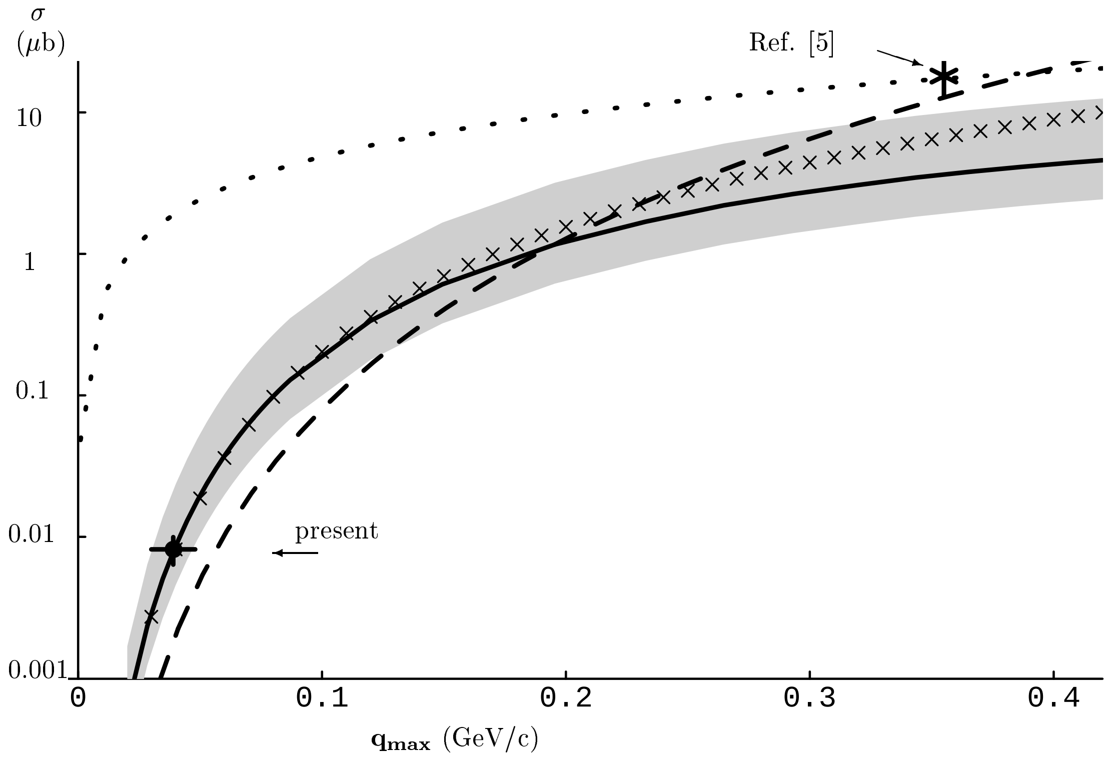

Figure 6: Cross section for the reaction $pp \longrightarrow pK^+\Lambda$ as function of the maximum momentum of K^+. Results based on Eq. 8 are shown as a solid line, where the shaded area depicts the uncertainty due to ambiguity in the normalization constant C. The crosses result from impulse approximation calculations by Fäldt and Wilkin. The dashed and the dotted lines represent the phenomenological parametrizations by Schürman (Eq. 4) and by Randrup (Eq. 5), respectively.

Here p is the relative momentum in the $N\Lambda$ CMS (i.e. $p = |\mathbf{p})$ and q is the kaon momentum in the three-body CMS. For fixed excess energy Q_{cm} these quantities are related by $p = \sqrt{2\mu(Q_{cm} - q^2/2\nu)}$ with $\mu = \frac{m_p \cdot m_\Lambda}{m_p + m_\Lambda}$ and $\nu = \frac{(m_p+m_\Lambda)\cdot m_K}{m_p+m_\Lambda+m_K}$. The maximum possible kaon momentum q_{max} is given by $q_{max} = \sqrt{2\nu Q_{cm}}$. The complete dynamical information about the process is contained in the reaction amplitude M.

Assuming the production amplitude M to be constant and neglecting the slowly changing $1/p_b$ term, one obtains from Eq. 3 that the production cross section σ is proportional to q^4_{max}. This behavior has been adopted by Schürmann and Zwermann [15] for the parametrization:

$$\sigma(\mu b) = 800 \cdot \left(\frac{q_{max}}{GeV/c}\right)^4, \tag{4}$$

which provides a reasonable fit [16] to the experimental data compiled in Ref. [17], i.e. for $q_{max} > 0.35\, GeV/c$. However, fig. 6 demonstrates that the q^4_{max} dependence is definitely not appropriate close to the kaon production threshold, since it underestimates the cross section of the present measurement significantly.

Note, that the parametrization (4) has been extensively employed in investigations of the kaon production in nucleon-nucleus and nucleus-nucleus collisions [18]. We also want to point out that the

					averaged values	
models	a_s (fm)	r_s (fm)	a_t (fm)	r_t (fm)	$\hat{a}$ (fm)	$\hat{r}$ (fm)
A [21]	-1.6	1.4	-1.6	3.2	-1.6	2.3
B [21]	-0.6	7.8	-1.9	2.4	-1.2	5.1
F [24]	-2.3	3.2	-1.9	3.4	-2.1	3.3
experiment						
[22]	-1.8	2.8	-1.6	3.3	-1.7	3.1
[23]	-2.0	5.0	-2.2	3.5	-2.1	4.3

Table 1: The N-Λ low energy scattering parameters for $^1S_0$ (s) and $^3S_1$ (t) partial waves.

parametrization linear in q_{max} given by Randrup and Ko [19],

$$\sigma(\mu b) = 24 \cdot \frac{q_{max}}{m_K} \ , \tag{5}$$

which is likewise commonly used in this context, overestimates the cross section in the threshold region by more than two orders of magnitude, as can also be seen in fig. 6.

The final state interaction between the two baryons introduces a significant energy dependence in the reaction amplitude. This is taken into account by Watson's model [20], where the reaction amplitude M is written as

$$|M|^2 \ = \ \frac{|M_0|^2}{p^2(1+\cot^2\delta)} \ . \tag{6}$$

Here $|M_0|^2$ is constant and δ is the S-wave phase shift, which is expressed by the effective range expansion

$$p \ cot\delta \ = \ -\frac{1}{a} + \frac{1}{2}rp^2 \ . \tag{7}$$

This model has been used successfully in explaining the energy dependence of the cross section for the reaction $pp \to pp\pi^0$ close to threshold [13], where the two protons are in $^1S_0$ final state. In the present case, the $p\Lambda$ system can contain two S-wave states, namely $^1S_0$ and $^3S_1$. Their amplitudes should be added incoherently. Experimental evidence [22, 23] as well as model calculations [21, 24] suggest that the scattering lengths and the effective ranges are rather similar for the singlet and triplet waves (cf. Table 1). Therefore, assuming the equality of effective range approximation parameters for both singlet and triplet states we obtain the formula for the total cross section with averaged values $(\hat{a}, \hat{r})$.

$$\sigma = \frac{C}{|\vec{p_b}|}\int_0^{q_{max}} \frac{p \cdot q^2}{p^2 + (-1/\hat{a} + \hat{r}p^2/2)^2} dq. \tag{8}$$

The normalization factor C, accommodating the amplitudes M_0 for singlet and triplet states, is treated as a free parameter.

In the present calculation we use the effective range parameters of model A from Table 1. The predicted energy dependence is shown by the solid line in fig. 6 where the curve has been normalized to our data point, yielding $C = 650^{+1100}_{-300} \ \ \mu b/(GeV/c)$. Due to the 0.1 % uncertainty in the determination of the beam momentum, there is a 20% error in q_{max} which results in a relatively large uncertainty of the energy dependence, as is indicated by the shaded area. Note that essentially all predictions based on effective range parameters from other models or experiments (as given by the values in Table 1) would lie within this shaded area.

The prediction of the simple S-wave model underestimates the experimental cross section for the BNL data point [5] at $q_{max} = 355\ MeV/c$. This is expected since P-waves (and possibly even higher partial waves) should contribute to the cross section in this energy range.
Moreover, the Σ^0 production channel, which opens at $q_{max} \approx 300$ MeV/c, may influence the Λ-hyperon production amplitude .

An alternative approach for taking into account the final state interaction betwen the two baryons has been proposed by G. Fäldt and C. Wilkin [25]. It predicts the energy dependence of the cross sections as shown by crosses in fig. 6. Up to a value of about q_{max} = 150 MeV/c these results are essentially identical to the ones shown by the straight line. We conclude that really more near threshold data are needed.

In a very recent work [26] an extended version of the resonance model [27], [28] was used to perform calculations for the energy dependence of the elementary kaon production cross sections. All relevant baryon resonances up to 2 GeV which decay into the kaon - hyperon channels were included in the relativistic consideration, but interference terms were neglected. These calculations underestimate the present data point by about one order of magnitude.

The calculations from Sibirtsev [29] for kaon production in heavy ion and proton - nucleus collisions used the elementary kaon production cross section in the one boson exchange model. Predictions of Ref. [29] appear to be in agreement to our present cross section value within a factor two.

4 Conclusion

The presented measurement is a first step. Further investigations are planned at the COSY facilities COSY-11 and COSY-TOF with the aim to measure the energy dependence of the $pp \longrightarrow pK^+\Lambda$ cross section, in order to extract information about both the p-Λ interaction at low energies as well as the reaction mechanism.

Based on the data point presented here, already two conclusions can be drawn: (i) parametrizations of the $NN \rightarrow N\Lambda K$ cross section as given by Randrup and Ko [19] and by Schürmann and Zwermann [15], which are commonly used in investigations of kaon production in nucleon-nucleus and nucleus-nucleus collisions, are definitely in disagreement with the present experimental data point at only 2 MeV above threshold and (ii) strong final state interaction in the p-Λ channel precludes the conjecture of the constant matrix element M in the vicinity of the reaction threshold.

Acknowledgements

During the preparation and the first runs of the COSY-11-Experiment we received support and encouragement from many sides. First of all we would like to express our deep gratitude to Prof.Dr.J.Treusch, his strong support of the whole COSY-Project and his enthusiasm for the research program was essential for the success also of the COSY-11-Experiment.

We appreciate long, inspiring and very helpful discussions with Prof. Dr. C. Wilkin.

The design and construction of the COSY-11 facility has profited a lot from know-how transfer between the two research centers CERN and Jülich, we would like to thank our friends at CERN for this cooperation.

We acknowledge the work provided by the COSY operation team for delivering the proton beam in a new machine. We appreciate the extensive work which has been done for the data acquisition system developed by people from the ZEL-KFA Jülich and the IKP-KFA Jülich.

The research project was supported by the BMBF, the Polish Committee for Scientific Research, and the Bilateral Cooperation Germany-Poland from the Stabsabteilung Internationale Beziehungen, Project Number XO81.15.

References

[1] A. Bravar et al., Phys. Rev. Let. 75 (1995) 3073

[2] J. Arvieux et al., 1991 Proposal 213 at Saturne

[3] P.D. Barnes et al., Phys. Rev. C to be published, and references therein.

[4] M. Bockhorst et al., Z.f.Physik C63 (1994) 37,
see in addition the planned experiments E-89-004, E-89-043 at CEBAF.

[5] W.J. Fickinger et al., Phys. Rev. 125 (1962) 2082

[6] R. Frascaria, Nuovo Cim. 102 (1989) 561

[7] Associated Strangeness Production in pp Reactions, Proposal 15-1 at COSY, 1988.
S.Wirth et al., Verhandlungen der DPG VI, 31 (1996) 940
Ch. Nake and A. Metzger, PhD theses to be published

[8] S. Brauksiepe et al., Nucl. Instr. and Meth. A 376 (1996) 397

[9] R. Maier et al., EPAC 94, Proc. of the Conf. (1994) 165

[10] K.A. Jenkins et al., Phys. Rev. D21 (1980) 2445

[11] D.T. Williams et al., Nuovo Cim. A8 (1972) 447

[12] R.A. Arndt, I.I.Strakovsky, R.L.Workman Phys. Rev. C50 (1994) 2731

[13] H.O. Meyer, Workshop on particle production near threshold, (Nashville, October 1990), AIP Conf. Proc. 221(1991) 129; H.O. Meyer et al., Nucl. Phys. A539 (1992) 633.

[14] E. Byckling, K. Kajantie, "Particle Kinematics", John Wiley & Sons, London 1973, page 50

[15] B. Schürmann and W. Zwermann, Phys. Lett. B183 (1987) 31.

[16] W. Zwermann, Mod. Phys. Lett. A3 (1988) 251.

[17] V. Flaminio et al., CERN-HERA 84-01

[18] G.Q. Li and C.M. Ko, Nucl. Phys. A594 (1995) 439, and references therein.

[19] J. Randrup and C.M. Ko, Nucl. Phys. A343 (1980) 519

[20] K.M. Watson, Phys. Rev. 88 (1952) 1163

[21] B. Holzenkamp et al., Nucl. Phys. A500 (1989) 485; A. Reuber et al., Nucl. Phys. A570 (1994) 543.

[22] G. Alexander et al., Phys. Rev. 173 (1968) 1452.

[23] B. Sechi-Zorn et al., Phys. Rev. 175 (1968) 1735.

[24] M.M. Nagels et al., Phys. Rev. D20 (1979) 1633.

[25] G. Fäldt and C. Wilkin, Phys. Lett. B382 (1996) 209.

[26] K. Tsushima, A. Sibirtsev, A.W. Thomas, Preprint ADP-96-29/T228

[27] K. Tsushima, S.W. Huang, A. Faessler, Phys. Lett. B337 (1994) 245

[28] K. Tsushima, S.W. Huang, A. Faessler, J.Phys. G21 (1995) 33

[29] A. Sibirtsev, Phys. Lett. B359 (1995) 29.